QCD Phase Structure and Anomalous Transport in a Chiral Environment as Seen in Lattice Experiments

V.V. Braguta[1,2], V.A. Goy[3], E.-M. Ilgenfritz[4], A.Yu. Kotov[5], A.V. Molochkov[3], M. Müller-Preussker[6], B. Petersson[6]

[1]Institute for High Energy Physics, Protvino, Russia,
[2]Far Eastern Federal University, School of Natural Sciences, Vladivostok, Russia,
[3]Far Eastern Federal University, School of Biomedicine, Vladivostok, Russia,
[4]Joint Institute for Nuclear Research, BLTP, Dubna, Russia,
[5]Institute of Theoretical and Experimental Physics, Moscow, Russia,
[6]Humboldt-Universität zu Berlin, Institut für Physik, Berlin, Germany

Brazil-JINR Forum “Frontiers in Nuclear, Elementary Particles, and Condensed Matter Physics”, Dubna, June 15-19, 2015

Outline

Outline

Outline

Outline

Outline

Outline

Outline

Outline

Brief history

- Around 2009/2010, a series of proof-of-concept studies of various magnetic field effects in QCD by lattice methods has started in the ITEP Lattice group, pioneered by M. I. Polikarpov († 2013) (using quenched LGT, mostly SU(2), partly SU(3, with overlap valence fermions).
- In 2010/2011, the study in non-quenched SU(2) LGT of the phase diagram with external magnetic field has independently started in the Berlin Phenomenology Group at Humboldt Universität.
- Following QCHS-X 2012, the decades-old Berlin-ITEP-JINR collaboration was extended to this new field. Until then, the collaboration was concentrated on the IR behaviour of gluon/ghost propagators and topological features at $T \neq 0$ (van Baal calorons, dyon mechanism of confinement and deconfinement).
- In 2014, the new field of collaboration has been geographically extended to the Far East Federal University Vladivostok.
  A lattice group has been inaugurated in Vladivostok last year.

Papers documenting the collaboration's start in 2014

1. Two-Color QCD with Non-zero Chiral Chemical Potential,
   V.V. Braguta, V.A. Goy, E. -M. Ilgenfritz, A. Yu. Kotov,
   A.V. Molochkov, M. Müller-Preussker, B. Petersson,
   arXiv:1503.06670 , just being published in JHEP
2. Study of the phase diagram of SU(2) quantum chromodynamics with nonzero chirality
   V.V. Braguta, V.A. Goy, E.-M. Ilgenfritz, A.Yu. Kotov,
   A.V. Molochkov, M. Müller-Preussker,
   JETP Lett. 100 (2015) 9, 547-549
   (Pisma Zh.Eksp.Teor.Fiz. 100 (2015) 9, 623-626)
3. Two-Color QCD with Chiral Chemical Potential
   V.V. Braguta, V.A. Goy, E.-M. Ilgenfritz, A. Yu. Kotov,
   A.V. Molochkov, M. Müller-Preussker, B. Petersson, A. Schreiber,
   contribution to Lattice 2014 (New York) and Quark Confinement and Hadron Spectrum XI (St. Petersburg), arXiv:1411.5174

Clarifications expected from Relativistic Heavy Ion Collisions

- Transition to a chirally symmetric and/or deconfined phase of QCD. What characterizes these two aspects partially/locally ?
- Existence of critical end point ? Existence of a first order line ?
- How is a dynamical description possible for the out-of-equilibrium process leading from the initial to the freeze-out stage ?
- May a better understanding of the equilibrium properties of the hydrodynamical phase (of almost chiral quasi-particles) help ?
- Why does QGP appear as a nearly ideal liquid ? How do the non-perturbative gluonic field configurations (monopoles) enforce the liquid-like behaviour ?
- More general: understanding of the QGP transport properties ?
- Fundamental QCD predicts "anomalous transport" phenomena under the influence of an external magnetic field of QCD scale $q\,H \sim O(1\ \mathrm{GeV}^2)$ in non-central A + A collisions.

Discoveries expected from Relativistic Heavy Ion Collisions: Anomaly-Induced Effects

- Manifestation of magnetically induced anomalous transport phenomena – a qualitatively new kind of discovery.
- The gravitational contribution to the QCD anomaly still awaits experimental confirmation (through the influence of vorticity formed in the partonic phase).
- The latter is closely related to the axial magnetic effect, which however plays no role in fundamental QCD, because no axial magnetic field exists on a fundamental level.
- However, this effect is proposed for condensed matter physics: in effective theories, Weyl fermions may experience magnetic field with different sign depending on helicity.

In other words, the QGP created in HIC might be considered as a show-case for a broad class of new "condensed matter physics" phenomena, in essence governed by the chiral anomaly.

Quantum Anomalies and Relativistic Hydrodynamics

- Hydro = effective low-energy theory, completely determined by conservation laws
- Conservation laws = consequences of symmetries of the underlying theory
- Some symmetries, however, are broken by quantum effects: the anomalies of QCD and QED
  - Chiral symmetry $\rightarrow$ axial anomaly
  - Scale symmetry $\rightarrow$ scale anomaly
- Anomalies introduce correlations between currents
- Classical background fields $\rightarrow$ collective motion in the Dirac sea
- Axial anomaly related to gauge field topology (Pontryagin index)

$$\partial_\mu \, J^\mu_A = 2 \, N_f \, Q(x) + \sum_f (2 i m_f) \, \bar{q}_f \, \gamma_5 \, q_f$$

$$Q(x) = \left(g^2 / 32 \pi^2 \right) \; G^a_{\mu\nu}(x) \, \tilde{G}^a_{\mu\nu}(x)$$

Chern-Simons Number

- topological density $=$ divergence of a topological (Chern-Simons) current

$$Q(x) = \partial^\mu \, K_\mu$$

$$K_\mu = \frac{1}{16\,\pi^2}\,\varepsilon_{\mu\alpha\beta\gamma}\left(A^a_\alpha\,\partial_\beta\,A^a_\gamma + \frac{1}{3}\,f^{abc}\,A^a_\alpha\,A^b_\beta\,A^c_\gamma\right)$$

- "prevacua" $|N_{CS}\rangle$ labelled by fixed Chern-Simons number

$$N_{CS}(x_0) = \int d^3\vec{x} K_0(x)$$

Prevacua separated by a periodic array of potential barriers.

- Actual vacuum (or thermal state) $=$ θ-vacuum (superposition)

$$|\theta\rangle = \sum_N \exp\left(i\theta N\right)|N\rangle$$

Special Chern-Simons Number Changing Processes

- instanton : tunneling in Minkowski time through a single barrier $N_{CS} \to N_{CS} \pm 1$
- sphaleron : "over-the-barrier" path at high temperature $N_{CS} \to N_{CS} \pm 1$
- glasma : a state of (anti)parallel color-magnetic and color-electric field, that continuously changes the Chern-Simon number

$$\frac{dN_{CS}}{dt} \propto B_i^a E_i^a$$

$$\frac{d(N_L - N_R)}{dt} = 2\, N_f\, \frac{dN_{CS}}{dt}$$

Outline

Chiral and Baryonic Chemical Potential Featuring in the Anomalous Transport Coefficients

$$\mu_B = (\mu_L + \mu_R)/2, \quad \mu_A = (\mu_L - \mu_R)/2 = \mu_5$$

- Chiral magnetic effect: $J_{V\mu} = \sigma_{VV} H_\mu, \quad \sigma_{VV} = \frac{\mu_A}{2\pi^2}$
- Axial chiral magnetic effect: $J_{A\mu} = \sigma_{AV} H_\mu, \quad \sigma_{AV} = \frac{\mu_B}{2\pi^2}$
- Chiral vortical effect: $J_{V\mu} = \sigma_V \omega_\mu, \quad \sigma_V = \frac{\mu_A \mu_B}{\pi^2}$
- Axial chiral vortical effect: $J_{A\mu} = \sigma_A \omega_\mu, \quad \sigma_A = \frac{\mu_B^2 + \mu_A^2}{4\pi^2} + \frac{T^2}{12}$

vorticity: $\omega_\mu = \frac{1}{2}\varepsilon_{\mu\nu\alpha\beta} u^\nu \partial^\alpha u^\beta$

vector and axial current: $J_V^\mu = n u^\mu \qquad J_A^\mu = n_5 u^\mu$

electric and magnetic field: $E^\mu = F^{\mu\nu} u_\nu \qquad H_\mu = \frac{1}{2}\varepsilon_{\mu\nu\alpha\beta}\, u^\nu\, F^{\alpha\beta}$

Chiral and Baryonic Chemical Potential and the Anomalous Transport Coefficients

anomalous transport coefficients $\rightarrow$ multiplied by $N_{\text{color}}\ q_f^2$ per flavour f

Explanation by Maxwell-Chern-Simons Theory

Extended Lagrangian of Maxwell-Chern-Simons electrodynamics

$$\mathcal{L}_{MCS} = -\frac{1}{4}F^{\mu\nu}F_{\mu\nu} - A_\mu J^\mu - \frac{c}{4}\theta\tilde{F}^{\mu\nu}F_{\mu\nu}$$

$$c = \sum_f \frac{q_f^2 e^2}{2\pi^2}$$

now coupled to QCD.
If $\theta =$ constant, the additional term $\theta\tilde{F}^{\mu\nu}F_{\mu\nu} = \theta\partial_\mu K^\mu$ is proportional to the (irrelevant!) full divergence of the Abelian Chern-Simons current:

$$K^\mu = \varepsilon^{\mu\nu\rho\sigma}A_\nu F_{\rho\sigma}$$

If $\theta = \theta(\vec{x}, t)$ (not constant), the term

$$\theta\tilde{F}^{\mu\nu}F_{\mu\nu} = \partial_\mu(\theta K^\mu) - (\partial_\mu\theta)K^\mu$$

leaves only $P_\mu = \partial_\mu\theta = (M, \vec{P})$ for a Chern-Simons term .....

Equations of Maxwell-Chern-Simons Theory

... in the electromagnetic action (coupling to QCD):

$$\mathcal{L}_{MCS} = -\frac{1}{4} F^{\mu\nu} F_{\mu\nu} - A_\mu J^\mu + \frac{c}{4} P_\mu K^\mu$$

Here, the pseudovector P_μ is fixed by the fluctuations of topological charge of colored fields (breaking Lorentz and rotational invariance), giving rise to essential modifications of the Maxwell theory:

$$\partial_\mu F^{\mu\nu} = J^\mu - P_\mu \tilde{F}^{\mu\nu}$$

$$\partial_\mu \tilde{F}^{\mu\nu} = 0$$

Modified Source Terms in Electrodynamics

electromagnetic current

$$\vec{j} \to \vec{j} + c\left(M\vec{B} - \vec{P} \times \vec{E}\right)$$

charge density

$$\rho \to \rho + c\vec{P} \cdot \vec{B}$$

If $\vec{P} = 0$, but $\dot{\theta} \neq 0$, external $\vec{B}$ with $\nabla \times \vec{B} = 0$ gives rise to an induced electromagnetic current

$$\vec{J} = -\frac{e^2}{2\pi^2}\,\dot{\theta}\vec{B}$$

$\dot{\theta}$ plays the role of the chiral chemical potential μ_5.

Why are Anomalous Transport Phenomena of Principal Interest ?

- They should be (in principle) expected in current heavy ion experiments, however difficult to disentangle in the final state.
- They are related to first principles of quantum field theory (originating from the chiral anomaly).
- They are macroscopic quantum phenomena shared by condensed matter systems, but hard to see in non-equilibrium HIC !
- They are non-dissipative phenomena (sustained in steady-state non-equilibrium under influence of magnetic field or vorticity).
- They are therefore accessible for usual Euclidean lattice simulations as if in equilibrium, however with $H \neq 0$.
- Axial chiral vortical effect is active even in case of $\mu_B = \mu_5 = 0$, which may be advantageous to simulate (without sign problem).

Axial Chiral Vortical Effect is formally related to Axial Magnetic Effect (related by the same Kubo formula)

Suppose (in addition to the gluon field) an Abelian axial magnetic field/vector potential coupling with opposite sign to both chiralities

$$S_f = \int \bar{\psi} \left(\partial_\mu \gamma_\mu - igA^a_\mu t^a \gamma_\mu - ie\gamma_5 A_{5\mu} \gamma_\mu \right) \psi.$$

An $A_{5\mu}$ with $\vec{H}_5 \neq 0$ creates a steady energy current $\vec{J}_\epsilon$ in the direction of the magnetic field with σ_A as transport coefficient:

$$J^i_\epsilon = \langle T^{0i} \rangle = \sigma_A H^i_5.$$

Effect visible in certain condensed matter systems (Weyl semi-metals) where a magnetic field can act like an axial magnetic field.
Observation of Axial Chiral Vortical Effect (ACVE) in HIC and Axial Magnetic Effect (AME) in condensed matter systems would mean confirmation of the gravitational contribution to the axial anomaly.

Lattice Confirmation of the Axial Magnetic Effect

1. Numerical evidence of the axial magnetic effect
   V. Braguta, M. N. Chernodub, K. Landsteiner, M. I. Polikarpov, M.V. Ulybyshev, Phys. Rev. D 88 (2013) 071501
2. Temperature dependence of the axial magnetic effect in two-color quenched QCD
   V. Braguta, M. N. Chernodub, V. A. Goy, K. Landsteiner, A. V. Molochkov, M. I. Polikarpov, Phys. Rev. D 89 (2014) 074510

- one has to check that $\vec{J}_\epsilon \propto \vec{H}_5, \quad J_\epsilon^{||} \propto |\vec{H}_5| \quad J_\epsilon^{\perp} \approx 0,$
- and measure the transport coefficient $C_{AME} = \frac{J_\epsilon}{eH_5 T^2} \neq 0$
- However, C_{AME} found smaller by than theoretically expected (still without renormalization of the energy momentum tensor !)
- Nonperturbative suppression with $T \to T_c + \varepsilon$ (towards the onset of quenched confinement) : $C_{AME}(T) = C_{AME}(\infty) \exp\left(-\frac{const}{T-T_c}\right)$

Lattice Confirmation of the Axial Magnetic Effect

A few technicalities:

- $H_5 =$ constructed as lattice curl of $A_{5\mu}$ (like usual H field)
- on a periodic lattice $\rightarrow$ usual flux quantization
- $A_{5\mu}(x)$ defines Abelian links $V_{x\mu} = \exp(i\,\theta_{x\mu})$, exactly as $A^{gluon}_{\mu}(x)$ defines non-Abelian $U_{x\mu}$
- $U^{QCD+QED}_{x\mu} = V_{x\mu}\; U_{x,\mu}$, i. e. Abelian $\times$ non-Abelian links
- $V_{x\mu}$ is non-dynamical !
- construction of the energy current

$$J^i_\epsilon = \langle T^{0i} \rangle = \frac{i}{2} \langle \bar{\psi} \left(\gamma^0 \; D^i_5 + \gamma^i \; D^0_5 \right) \psi \rangle$$

Lattice Confirmation of the Axial Magnetic Effect

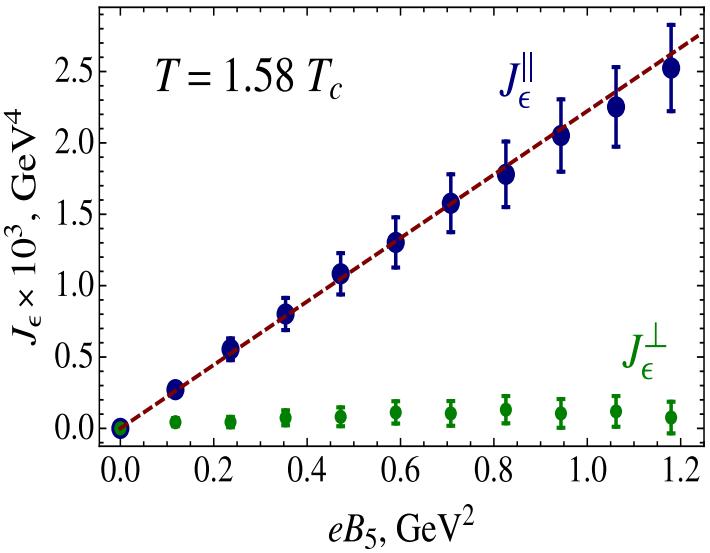

observe $J_\epsilon \propto H_5$
extract coefficient C_{AME}

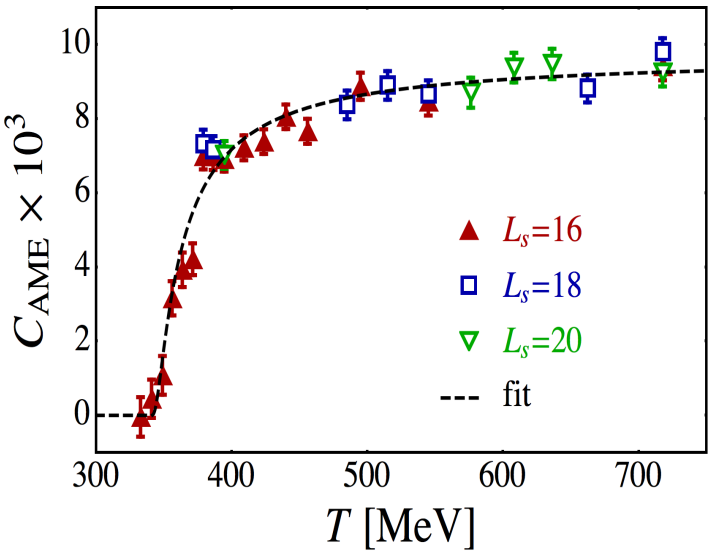

find $C_{AME} \to 0$
for $T \to T_c + \varepsilon$

Outline

Chiral Chemical Potential Appearing in the Action

$$S_f = \int \bar{\psi} \left(\partial_\mu \gamma_\mu - igA^a_\mu t^a \gamma_\mu + m + \mu_5 \gamma_0 \gamma_5 \right) \psi$$

$$n_5 = a^3 \langle \bar{\psi} \gamma_0 \gamma_5 \psi \rangle = a^3 \langle \psi^\dagger_R \psi_R - \psi^\dagger_L \psi_L \rangle > 0$$

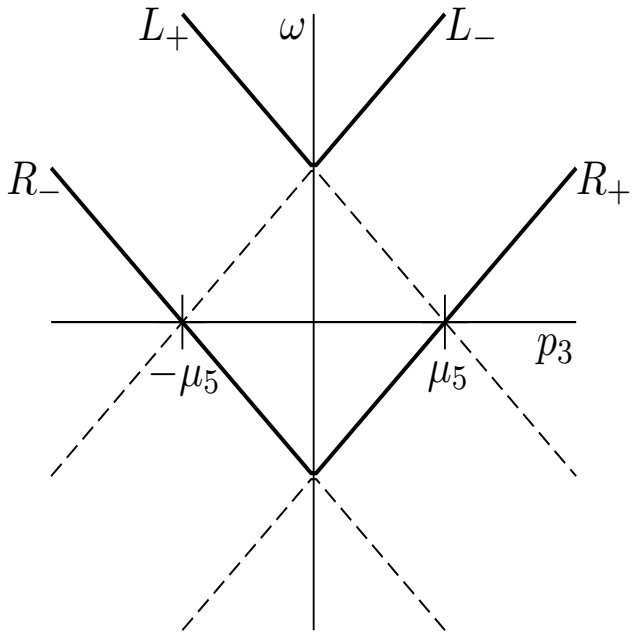

"chirally imbalanced matter"

Fukushima, Kharzeev, Warringa: arXiv:0808.3382

Local Fluctuations of Topological Charge Density

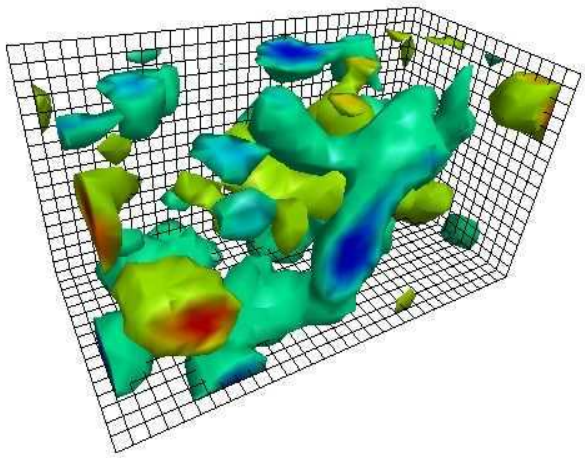

fermionic topological density
$\lambda_{\text{cut}} = 634$ MeV

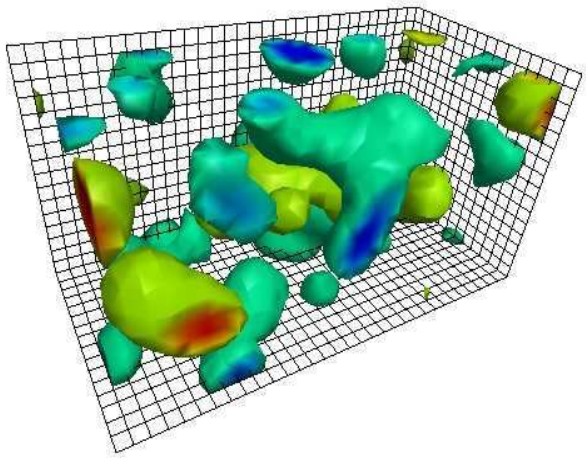

gluonic topological density
48 sweeps of "Wilson flow"

Topological charge density of a $T = 0$ configuration with $Q = 0$

E.-M. I., D. Leinweber, P. Moran, K. Koller, G. Schierholz, V. Weinberg, Phys. Rev. D77 (2008) 074502

At high T, similar but more fine-grained fluctuations form a diffusion constant $\Gamma \simeq 30\ \alpha_s^4\ T^4 \rightarrow$ responsible for washing out of $n_5 \neq 0$ which would be growing with time (event-wise) from a classical "glasma"

Possible Origin of Topological Charge in HIC

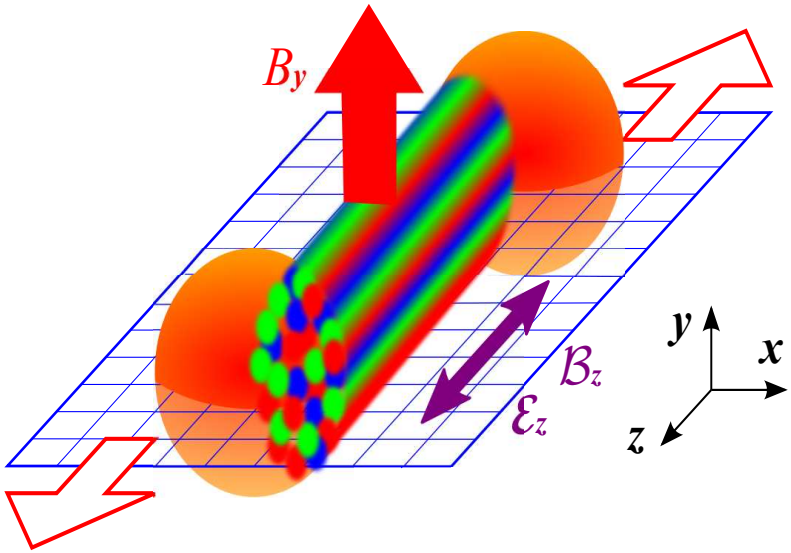

color flux tube with parallel color-electric and color-magnetic fields

Fukushima, Kharzeev, Warringa: arXiv:1002.2495

Schwinger-mechanism for quark-pair production from the tube:

$$\partial_t j_y = \frac{q^2 B_y}{2\pi^2} \frac{g \mathcal{E}_z \mathcal{B}_z^2}{\mathcal{B}_z^2 + \mathcal{E}_z^2} \coth\left(\frac{\mathcal{B}_z}{\mathcal{E}_z}\pi\right) \times \exp\left(-\frac{2 m^2 \pi}{|g \mathcal{E}_z|}\right)$$

with

color-electric/magnetic fields $\mathcal{E}_z$, $\mathcal{B}_z$, electromagnetic fields $\vec{E}, \vec{B}$

How Actually the Charge Flux Asymmetry Emerges

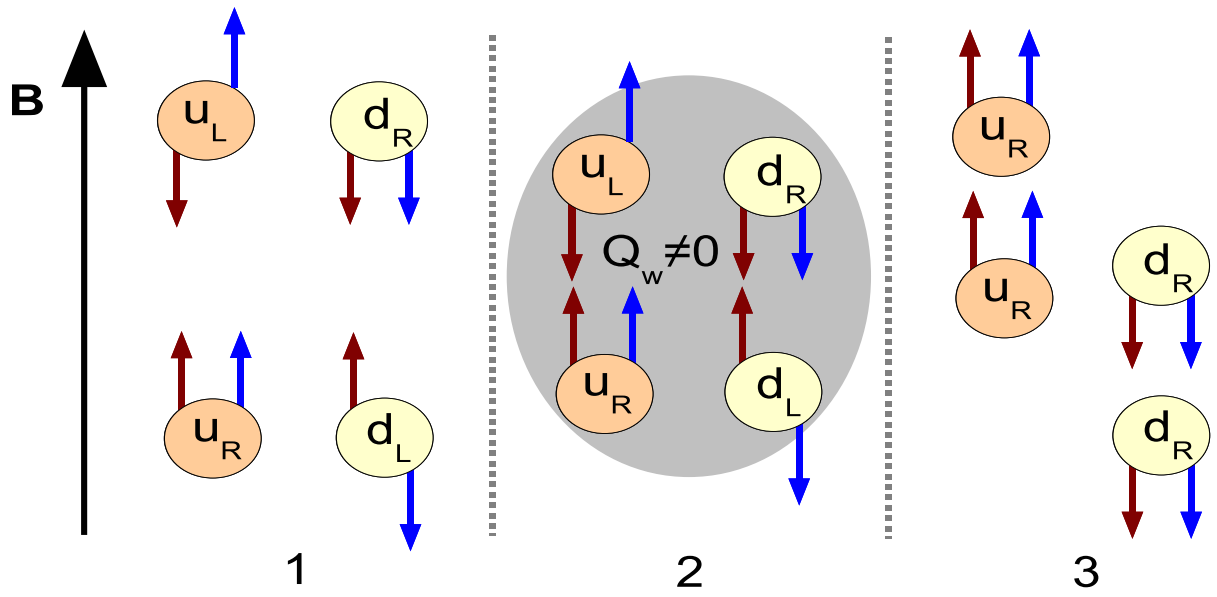

local topological charge transformed into charge separation

Kharzeev, arXiv:0711.0950

red arrows = momentum and blue arrows = spin

left: left-right symmetric state, right: more right- than left-handed

Origin of the Electro-Magnetic Field in HIC

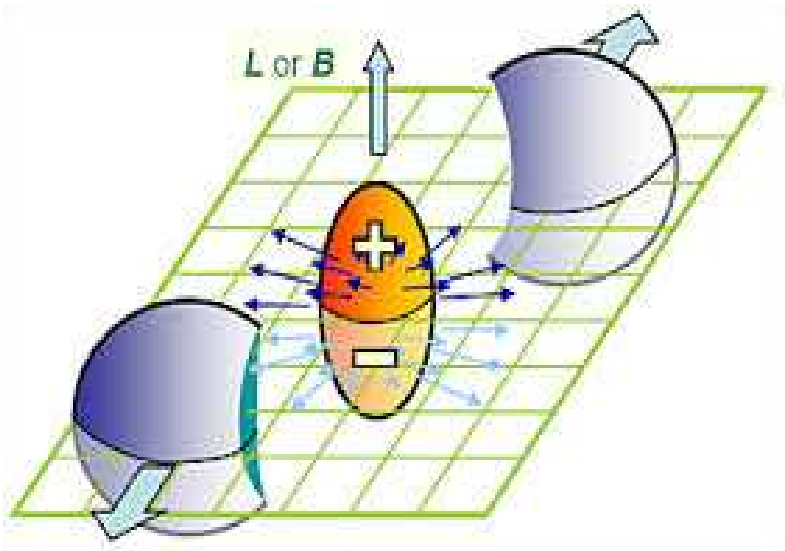

(mainly) spectator nucleons generate the magnetic field

- CME only one among other μ_5-induced non-dissipative effects !
- All these effects become operative in the deconfinement phase (in the plasma state).
- Therefore, it is important to explore the μ_5–T phase diagram.
- Contrary to μ_B, chiral μ_5 is not afflicted by the sign problem.
- Thus, plain hybrid Monte Carlo lattice simulation is possible.

Outline

Phenomenological Studies of Phase Structure

1. M. N. Chernodub and A. S. Nedelin, Phase diagram of chirally imbalanced QCD matter,
   Phys. Rev. D**83**, 105008 (2011), arXiv: 1102.0188(hep-ph)
2. K. Fukushima, M. Ruggieri and R. Gatto, Chiral magnetic effect in the PNJL model,
   Phys.Rev. D**81**, 114031(2010), arXiv:1003.0047(hep-ph)
3. A. A. Andrianov, V. A. Andrianov, D. Espriu, X. Planells, Chemical potentials and parity breaking: the Nambu-Jona-Lasinio model,
   Eur. Phys. J. C**74**, 2776 (2014), arXiv: 1310.4416(hep-ph)

Prediction of the Linear σ Model with Polyakov Loop

M. N. Chernodub and A. S. Nedelin, Phase diagram of chirally imbalanced QCD matter,
Phys. Rev. D**83**, 105008 (2011), arXiv: 1102.0188(hep-ph).

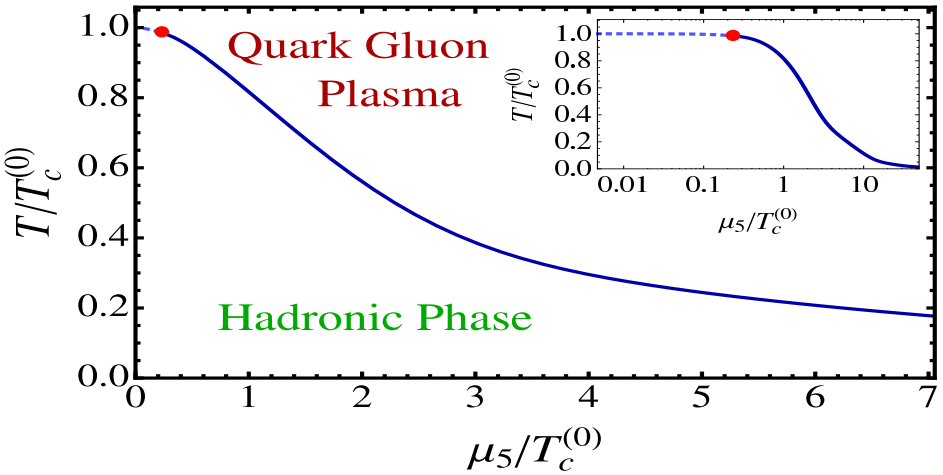

μ_5 dependence of T_c

The crossover turns into a first order transition at moderate μ_5.
T_c is predicted to decrease at larger μ_5.
Qualitatively similar to the effect of baryonic chemical potential μ_B.
All effective-model papers differ in details (chiral condensate vs μ_5).

Outline

Other Lattice Studies with Chiral Chemical Potential

There were earlier lattice studies of the Chiral Magnetic Effect (actually tests of $j \propto H$) where a lattice implementation of μ_5 adequate for Wilson fermions and a lattice implementation of H was used. However, the μ_5-dependence of the crossover temperature T_c was not systematically studied in these papers.

- Chiral magnetic effect in lattice QCD with a chiral chemical potential,
  Arata Yamamoto, Phys. Rev. Lett. 107 (2011) 031601,
  arXiv:1105.0385
- Lattice study of the chiral magnetic effect in a chirally imbalanced matter,
  Arata Yamamoto, Phys. Rev. D84 (2011) 114504,
  arXiv:1111.4681
- Chiral Magnetic Effect on the Lattice,
  Arata Yamamoto, Lect. Notes Phys. 871 (2013) 387-397,
  arXiv:1207.0375

Lattice Studies of the Chiral Magnetic Effect

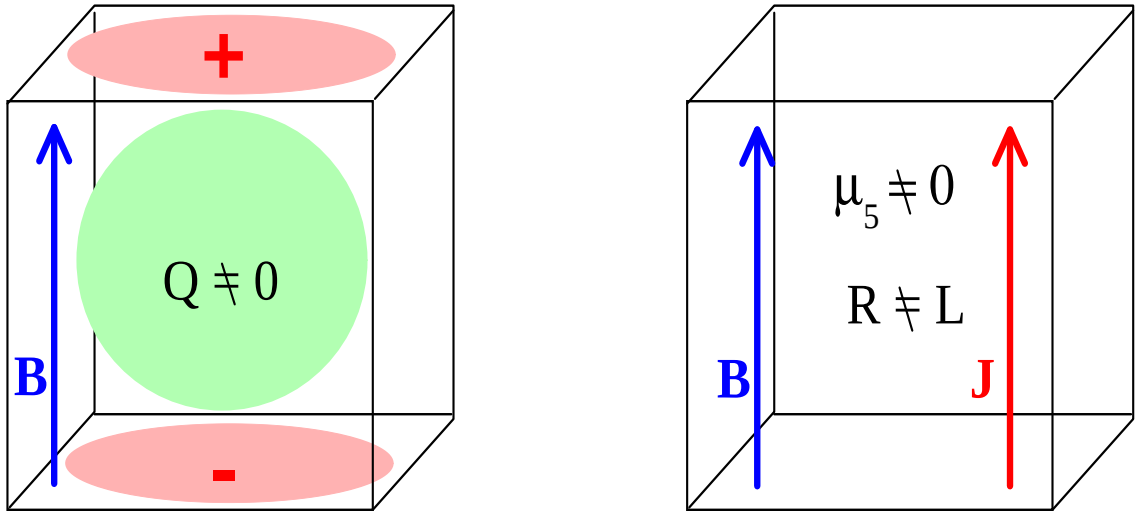

Figure: left: (early papers) with a prepared topological background field Q, right: (more recently) with $\mu_5 \neq 0$

Two settings for lattice studies of the Chiral Magnetic (also known as "Charge Separation") Effect.

Yamamoto, arXiv:1207.0375

The Aim of this Study with Dynamical Quarks :

The first task to start with:

fixing the phase diagram of QCD in the μ_5–T plane
(of chiral chemical potential and temperature)
by a non-quenched lattice simulation

Two-Color QCD with Non-zero Chiral Chemical Potential,
V.V. Braguta, V.A. Goy, E. -M. Ilgenfritz, A. Yu. Kotov,
A.V. Molochkov, M. Müller-Preussker, B. Petersson,
arXiv:1503.06670 , just being published in JHEP

Our Simulation Code

The code was developed on the basis of the CUDA code (for GPU) written by A. Schreiber, Humboldt University, Berlin, for the project to study the H–T phase diagram. Corresponding results have been published in:

- E.-M. I., M. Kalinowski, M. Müller-Preussker, B. Petersson, A. Schreiber,
  Two-color QCD with staggered fermions at finite temperature under the influence of a magnetic field
  Phys.Rev. D**85** (2012) 114504, arXiv: 1203.3360
- E. -M. I., M. Müller-Preussker, B. Petersson, A. Schreiber,
  Magnetic catalysis (and inverse catalysis) at finite temperature in two-color lattice QCD
  Phys.Rev. D89 (2014) 5, 054512, arXiv: 1310.7876

Computational Resources used for this Project

The actual simulations for no-zero chiral chemical potential were performed at GPUs of

- the K100 supercomputer of the Institute of Applied Mathematics, Russian Academy of Science, Moscow,
- the computers of the Particle Phenomenology Group at Humboldt Universität Berlin.

Side remark on computing resources to our disposal :
Another Berlin-JINR collaboration (with A. Trunin, BLTP), concerning the present tmfT ongoing topic "Twisted mass lattice thermodynamics with $N_f = 2 + 1 + 1$ flavors" (EoS, topology, screening, transport etc.), is making use of the GPUs of

- "Lomonosov" Supercomputer of Moscow State University,
- "Korolyov" Supercomputer at Aero-Space University Samara,
- "HybriLIT" heterogenous computing facility at JINR's LIT,

besides of resources in Germany (HLRN, Humboldt).

Implementation of Chiral Chemical Potential on the Lattice

- For Wilson fermions obvious (Yamamoto)
- Implementation for staggered fermions:

$$S_f = \frac{1}{2}\sum_{x\mu}\eta_\mu(x)(\bar{\psi}_{x+\mu}U_\mu(x)\psi_x - \bar{\psi}_x U^\dagger_\mu(x)\psi_{x+\mu}) + ma\sum_x \bar{\psi}_x\psi_x +$$

$$+\frac{1}{2}\mu_5 a\sum_x s(x)(\bar{\psi}_{x+\delta}U_{x+\delta,x}\psi_x - \bar{\psi}_{x+\delta}U^\dagger_{x+\delta,x}\psi_x)$$

Here
$\bar{\psi}_x$, ψ_x a pair of colored Grassmann fields (each color represented by a one-component spinor)
$\delta = (1,1,1,0)$ equal-time shift vector in the 2^4 elementary cell
$s(x) = (-1)^{x_2}$ corresponds to $\gamma_0\gamma_5$ (together with the shift)
$U_{x+\delta,x}$ is a product of gauge links along the paths $x \to x+\delta$ (appropriately averaged over 6 different paths)

Our Lattice Setup

- $SU(2)$ gauge group (for simplicity taken from the H-T project)
- For gauge fields we adopted the Wilson action

$$S_g = \frac{\beta}{4} \sum_{x,\mu\neq\nu} tr\left(1 - U_\mu(x)U_\nu(x+\mu)U_\mu^\dagger(x+\nu)U_\nu^\dagger(x)\right)$$

- 4 "tastes" of dynamical staggered fermions (here without rooting).
- 5 values of μ_5: 0, 150, 300, 475, 950 MeV.
- lattice size 6×20^3, partly 10×28^3 (this allows to go to larger μ_5).
- small quark mass $m \approx 12$ MeV ($m_\pi \approx 330$ MeV) or $m \approx 18.5$ MeV ($m_\pi \approx 550$ MeV), respectively.
- For each (β, μ_5) point $N_{\text{configurations}} \sim O(10000)$ (small lattice) or $N_{\text{configurations}} \sim O(1000)$ (large lattice) have been produced, respectively.

Order parameters

- Polyakov loop $\langle L \rangle$:

$$L = \frac{1}{N_\sigma^3} \sum_{n_1,n_2,n_3} \frac{1}{2} tr \left(\prod_{n_4=1}^{N_\tau} U_4(n_1, n_2, n_3, n_4) \right)$$

- Chiral condensate $a^3 \langle \bar{\psi}\psi \rangle$:

$$a^3 \langle \bar{\psi}\psi \rangle = -\frac{1}{N_\tau N_\sigma^3} \frac{1}{4} \frac{\partial}{\partial(ma)} \log(Z) = \frac{1}{N_\tau N_\sigma^3} \frac{1}{4} \langle Tr(D + ma)^{-1} \rangle$$

In this study, Polyakov loop and chiral condensate have been left unrenormalized.

Corresponding Susceptibilities

- Polyakov loop susceptiblity:

$$\chi_L = N_\sigma^3(\langle L^2\rangle - \langle L\rangle^2)$$

- Chiral susceptibility (disconnected part):

$$\chi = \frac{1}{N_\tau N_\sigma^3}\frac{1}{16}(\langle(Tr(D+ma)^{-1})^2\rangle - \langle Tr(D+ma)^{-1}\rangle^2)$$

Outline

Our Lattice Results: Polyakov Loop and Chiral Condensate

Lattice results for 6×20^3 and quark mass $m \approx 12$ MeV.

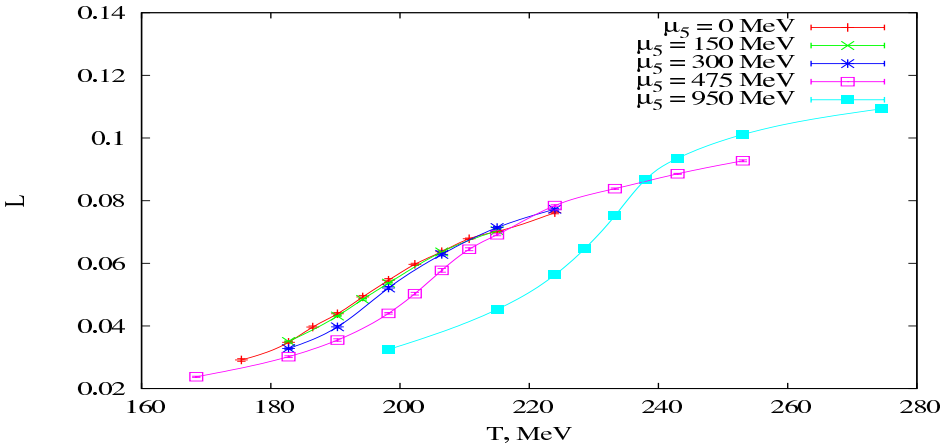

Polyakov loop

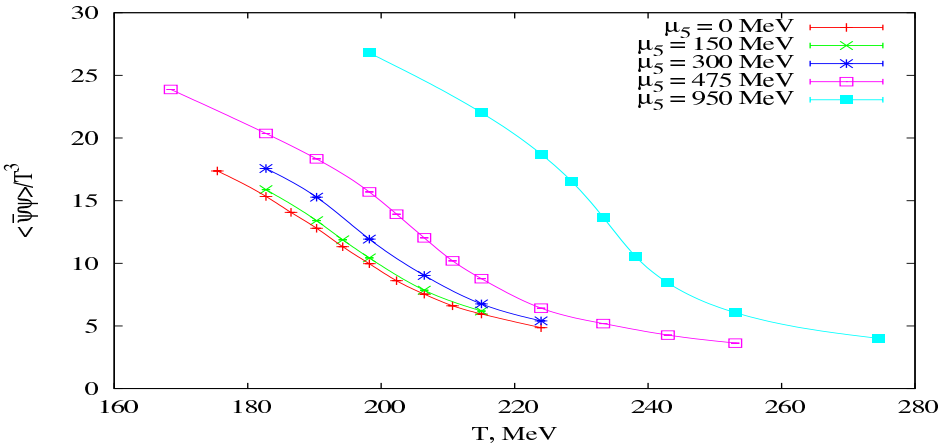

chiral condensate

Figure: Polyakov loop and chiral condensate versus T for five values of μ_5 on the small lattice.

Our Lattice Results: Polyakov Loop Susceptibility and Chiral Susceptibility

Lattice results for 6×20^3 and quark mass $m \approx 12$ MeV.

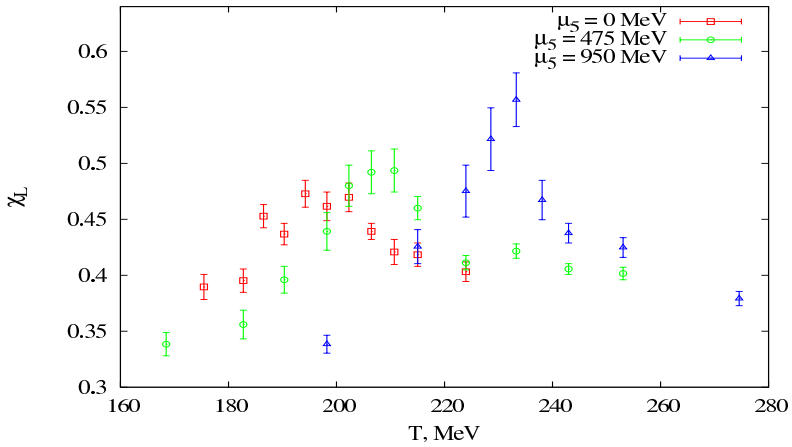

Polyakov loop susceptibility

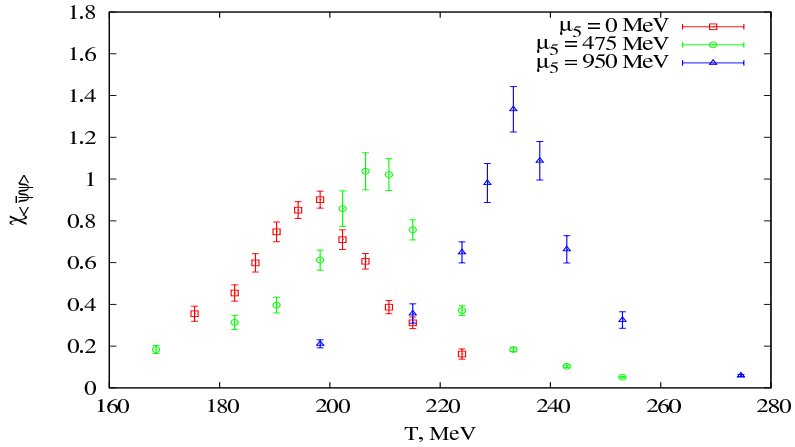

chiral susceptibility

Figure: Polyakov loop susceptibility and chiral susceptibility versus T for three values of $\mu_5 = 0, 475, 950$ MeV.

Our Lattice Results: Polyakov Loop Susceptibility and Chiral Susceptibility

Lattice results for 6×20^3 and quark mass $m \approx 12$ MeV.

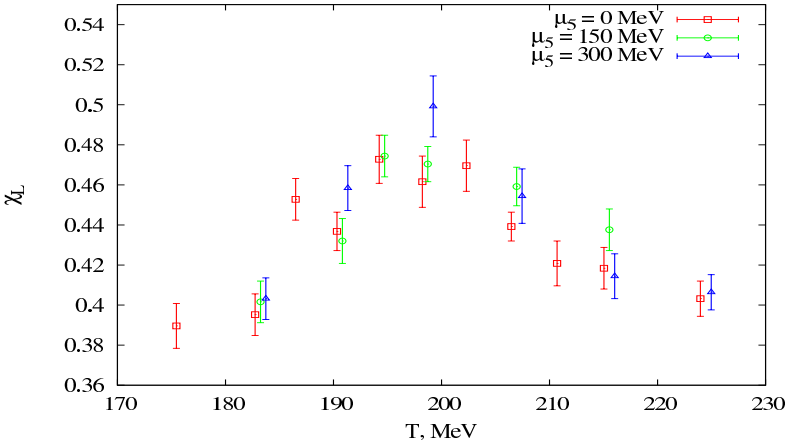

Polyakov loop susceptibility

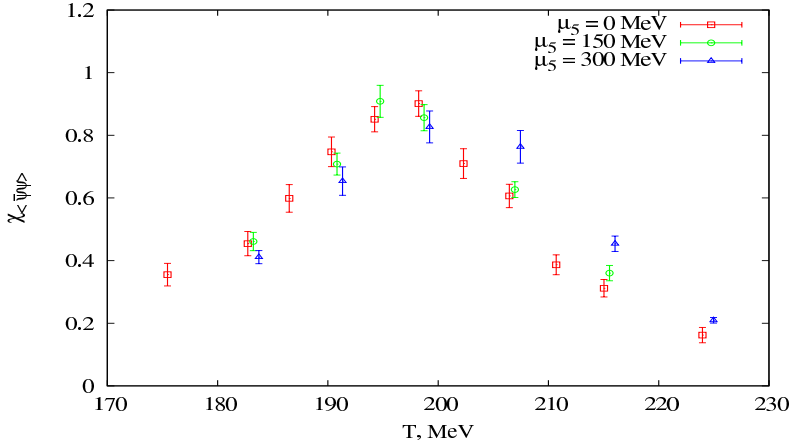

chiral susceptibility

Figure: Polyakov loop susceptibility and chiral susceptibility versus T for μ_5 with a smaller increment at lower values $\mu_5 = 0, 150, 300$ MeV.

Dependence of T_c on the Chiral Chemical Potential μ_5

μ_5 (MeV)	β_c	T_c (MeV)
0	1.7975 ± 0.0005	195.8 ± 0.4
150	1.7984 ± 0.0009	196.7 ± 0.7
300	1.8012 ± 0.0007	198.9 ± 0.5
475	1.8116 ± 0.0003	207.5 ± 0.2
950	1.8404 ± 0.0002	233.3 ± 0.2

The critical temperature T_c and the inverse lattice gauge coupling β_c as a function of the chiral chemical potential μ_5 obtained from a Gaussian fit of the chiral susceptibility near the peak

$$\chi = a_0 + a_1 \exp\left(-\frac{(\beta - \beta_c)^2}{2\sigma^2}\right).$$

The susceptibilities were taken from simulations at 6×20^3 lattices with quark mass $m \approx 12$ MeV.

Dependence of T_c on the Chiral Chemical Potential μ_5

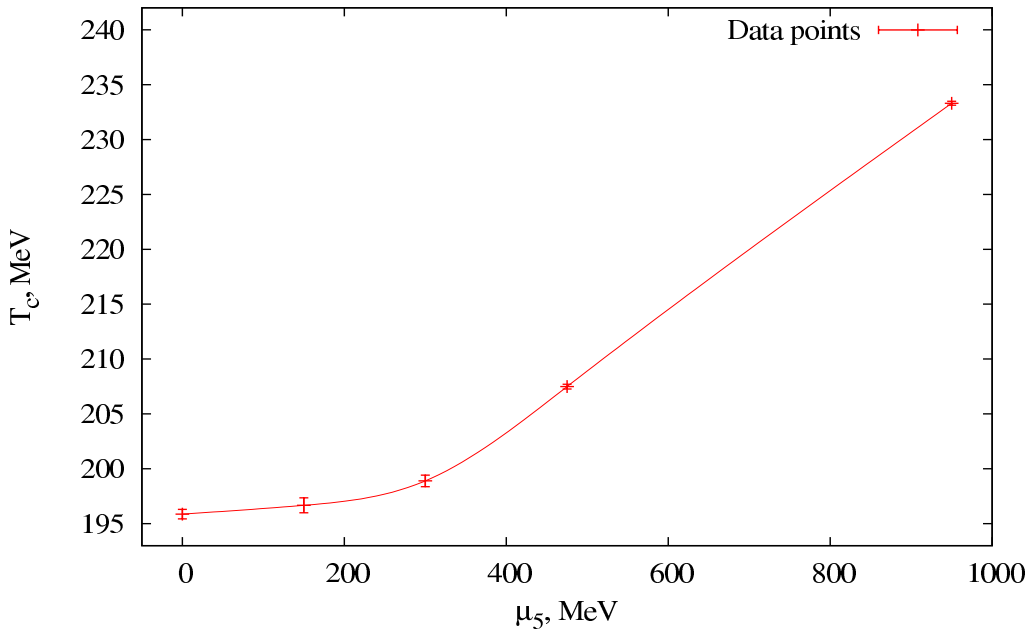

Figure: The critical temperature T_c as function of the chiral chemical potential μ_5,as obtained on the 6×20^3 lattice with quark mass $m \approx 12$ MeV.

Our Lattice Results on a Bigger/Finer Lattice: 10×28^3

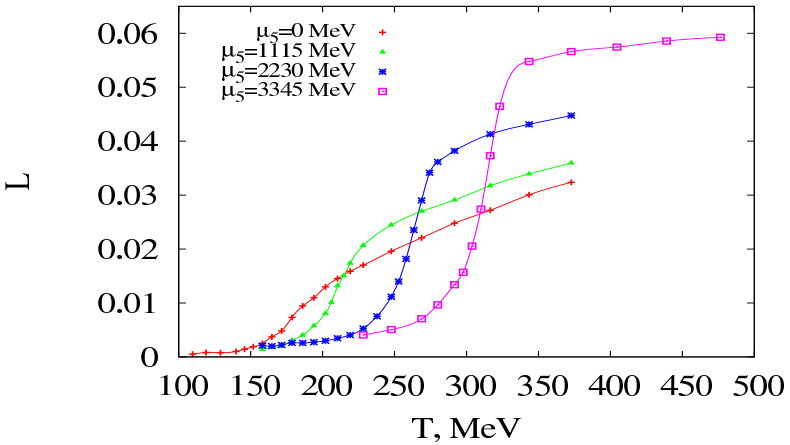

Polyakov loop

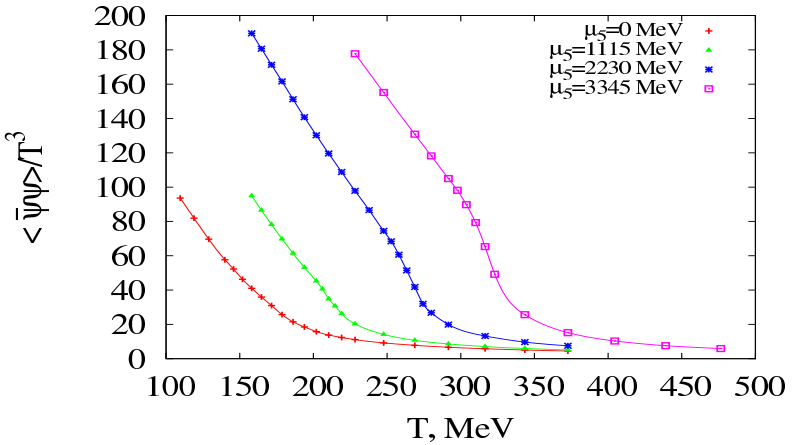

chiral condensate

Figure: Polyakov loop and chiral condensate versus T for 4 values of $\mu_5 = 0, 1115, 2230, 3345$ MeV on the large lattice. The quark mass is $m \approx 18.5$ MeV.

The transition becomes sharper with smaller lattice spacing and with increasing μ_5.
So far, no susceptibilities have been measured at the bigger lattices !

Polyakov Loop and Chiral Condensate vs. μ_5, for Different Temperature Ranges

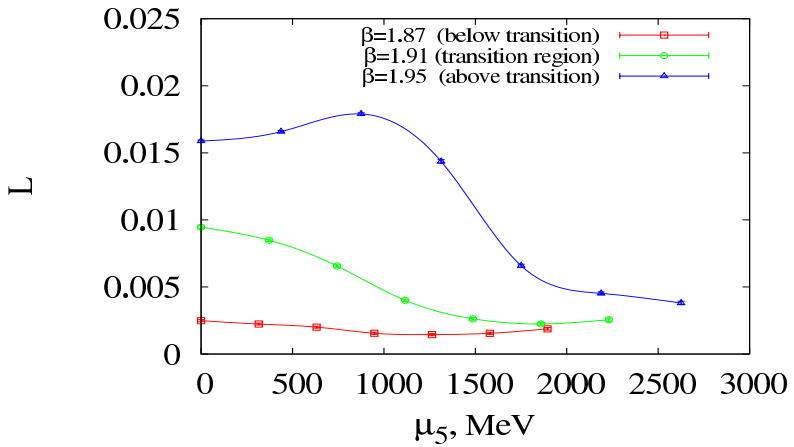

Polyakov loop

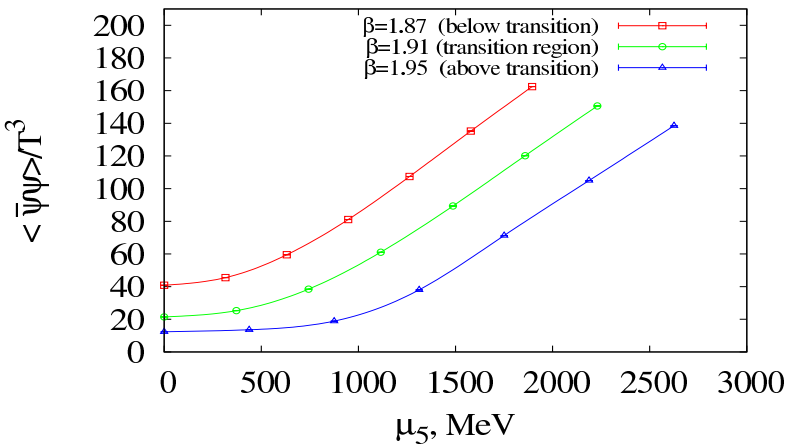

chiral condensate

Figure: Polyakov loop and chiral condensate versus μ_5. The lattice data are taken from 10×28^3 with quark mass $m \approx 18.5$ MeV.

The characteristic behavior is shown for three temperature regimes: below transition, within the transition region and above transition.

μ_5 Dependence : Interpretation

- Polyakov loop/confinement aspect: If at $\mu_5 = 0$
  - the system is in the confinement phase, it remains so with increasing μ_5.
  - the system is in deconfinement phase, it increases the deconfining property, before it goes to confinement.
  - the system is in the transition region, it goes immediately to confinement with increasing μ_5.
- Chiral symmetry breaking (for non-zero quark mass): If at $\mu_5 = 0$
  - the system is in the strongly broken phase, it becomes even stronger so with increasing μ_5.
  - the system is in the chirally nearly restored phase (deconfinement phase), it becomes chirally broken later, at higher μ_5.
  - the system is in the transition region, chiral symmetry breaking grows immediately with increasing μ_5.

Chiral Limit of the Chiral Condensate at Different μ_5 for 4 Different Temperatures

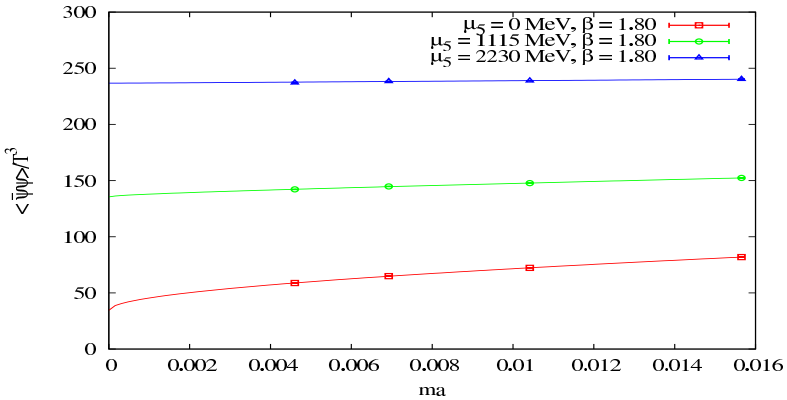

confinement phase

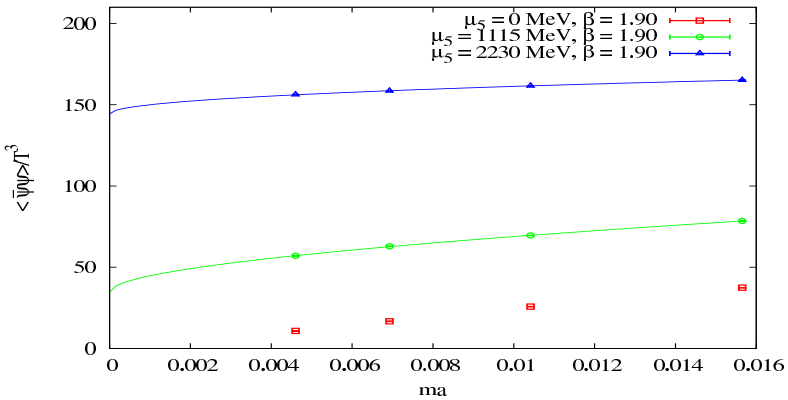

transition region

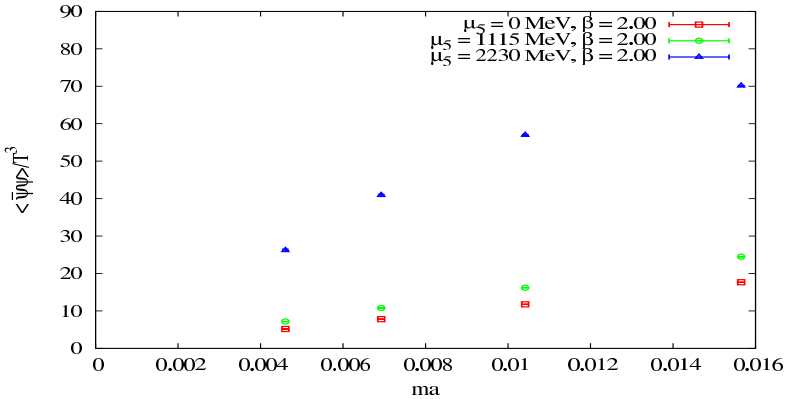

upper transition region

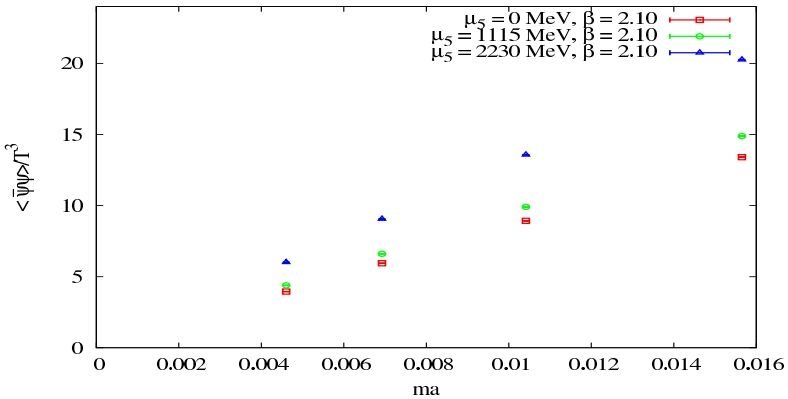

deconfinement phase

Ciral limit $m \to 0$: Interpretation

- Polyakov loop/confinement aspect:
  The mass dependence of the Polyakov loop is not characteristic, for all temperature and μ_5 regions (not shown).
- Chiral condensate in the limit $m \to 0$
  - low temperature region: the chiral condensate has a non-zero limit
    at $m \to 0$; this limit rises with increasing μ_5.
  - high temperature region ($\beta = 2.10$ and $\beta = 2.20$):
    the chiral condensate behaves compatible with a vanishing limit for $m \to 0$; the slope increases with μ_5 and decreases with temperature.
  - transition region: the chiral condensate has a non-zero limit at $m \to 0$ only for $\mu_5 = 0$; otherwise the limit grows with μ_5.

Outline

Conclusions

- T_c was found slightly inreasing with increasing μ_5.
- The “transition” (actually a crossover) becomes steeper with smaller lattice spacing (for that larger lattices are needed).
- This tendency is contrary to the first phenomenological studies: effective PNJL, PLσM etc.
- Other phenomenological studies support the tendency found here: Schwinger-Dyson approach (gluon propagators) and large-N_{color} arguments (analogy isospin chemical potential, π-condensation).

Outlook

Left for upcoming work:

- Evaluation of chiral density and of the topological structure (influence on the topological susceptibility).
- Re-introducing a magnetic field (chiral magnetic effect).
- Replacement SU(2) by SU(3) gauge group.
- Introducing of "rooting": allows a free choice of N_f, of masses and of charges.
  In particular, $N_f = 2$ (as in effective models) will be addressable.
- Renormalization of observables: Polyakov loop, chiral condensate(s), energy-momentum tensor, fluxes ...